CORM: Constrained Optimal Reconfiguration Matrix for Safe On-Ramp Cooperative Merging of Automated Vehicles

Lyes Saidi, Lounis Adouane, Reine Talj

CORM: Constrained Optimal Reconfiguration Matrix for Safe On-Ramp Cooperative Merging of Automated Vehicles

Lyes Saidi [1], Lounis Adouane [1] and Reine Talj [1]

Abstract— **On-ramp cooperative merging maneuver is currently one of the most challenging tasks for cooperative and automated vehicles (CAVs). Safety concern is the key aspect to capture the performance of the merging strategy. In this paper, it is proposed to adapt the dynamic inter-target distance matrix originally developed in [13] in order to explicitly integrate the environmental constraints (e.g., road borders). The main objectives of the proposed Constrained Optimal Reconfiguration Matrix (CORM) are to ensure safe and reliable navigation of the CAVs in formation and guarantee a smooth merging maneuver, while taking into account the on-road environment constraints. An analytical model of the formation composed by the CAVs is presented, in addition to a formal demonstration of the respect of the in-between distances using the constrained optimal reconfiguration matrix. Simulations in different scenarios are performed to evaluate the safety and the efficiency of the proposed approach.**

I. INTRODUCTION

An important amount of the current researches in the area of autonomous vehicles (AVs) concerns the methods and tools to guarantee on road safety. However, a number of situations will compulsory require coordinating the relative motions of the AVs to ensure the zero-collision requirement [1]. One of the most active research topics corresponds to autonomous and cooperative navigation of a group of vehicles, also known as navigation in formation control [13]. In fact, cooperative navigation advantages deals with several intelligent transportation system (ITS) topics, such as: safety with accident reduction, health while improving passengers comfort, transportation time since it reduces road congestion, ecology with fuel efficiency among other advantages [1]. The authors in [2] highlighted the navigation in formation and cooperative maneuvers capabilities in terms of energy saving and its consequences on the other driving aspects (e.g., traveling time, comfort). In this paper, we are particularly interested on the safety related improvement that can be obtained using a cooperative and formation based approach.

Coordinating the movement and activities of the Cooperative and Automated Vehicles (CAVs) in a formation is a very vast problem, including a wide variety of scenarios: from cruise and merging management, where maneuvers like cooperative merging on-ramp can be seen in [3], so as tools like Cooperative Adaptive Cruise control (CACC) [4], used for platoon control, to scenarios like cooperative intersection crossing [5].

In this paper, we aim to take advantage from the cooperative formation control to tackle the challenging scenario of on-ramp merging performed by Cooperative and Automated Vehicles (CAVs) [3][8][11]. The difficulty arises for the CAV along the on-ramp, where it has to discern whether to accelerate or decelerate to enter the main line safely. Meanwhile, the mainline users may have to modify their speeds to permit the entrance of the merging CAV, thus affecting traffic flow which may result in road congestion.

One solution to tackle the on-ramp merging consists of considering the CAVs that participate in the merging maneuver as a formation. For this aim, we propose to adapt the formulation proposed in [13] originally designed for open area scenario to the considered scenario in this paper, while taking into account the on-road scenario constrains. The adaptation is based on the proposed Constrained Optimal Reconfiguration Matrix (CORM). The latter is based on an optimization algorithm, used to compute the most suitable convergence of the formation from the triangular merging shape toward the desired linear shape. In the meantime, the proposed CORM algorithm guarantees the safety of the maneuver with respect to the formation participants and the road geometry.

The remainder of the paper is organized as follows. In Section II, the related work to the on-ramp merging scenario, and the objectives of this paper are discussed. In Section III, we introduce the preliminaries and the problem formulation. Section IV details the proposed CORM algorithm. In Section V, we present the conducted simulations. We draw conclusions and set perspectives in Section VI.

II. RELATED WORK AND OBJECTIVES

When addressing on-ramp merging scenario with a cooperative approach, two main topics are generally addressed: (a) the modeling of the group of vehicles that participate in the merging maneuver, and (b) the motion coordination approach used to define the passing order and orchestrate the movements of the CAVs. In this section, a brief overview of the existing approaches for formation modeling and control are presented. Motion coordination based on consensus-based control is discussed among other motion coordination methods. Finally, the objective and the main contribution of this paper are presented.

Based on the communication range of the CAVs (cf. Figure 2), the vehicles participating in the merging maneuver can be identified to create a formation. The formation modeling is a largely discussed topic in the literature. In [6], the authors conducted a comprehensive survey related to the leader-follower formation modeling approach. The main advantage of this approach is its simplicity. However, its dependence

The authors are with:
[1]Université de technologie de Compiègne (UTC), CNRS, Heudiasyc, 60200 Compiègne, France. FirstName.LastName@hds.utc.fr

on the leader corresponds to its main drawback. The virtual structure approach for formation modeling was proposed to overcome the leader follower approach drawbacks. Based on the CAVs positions, the shape of the virtual structure is defined, and depending on the desired motion, the distances between the vehicles can be adjusted easily using virtual targets computed to maintain the desired shape [7]. According to [13], the advantage of this approach is its flexibility w.r.t. the participating vehicles number and the type of the desired maneuver. In this paper, the virtual structure approach is used to model the formation composed of the CAVs that participate in the merging maneuver. This choice is mainly motivated by the safety requirement. In fact, the virtual structure permits to model the formation formally and to control easily the in-between distances within the formation.

The goal of the motion coordination is to safely synchronize the motion of the CAVs, part of the formation, in order to respect a certain passing order of the CAVs in the merging zone (cf. Figure 2). The work given in [8] explains the challenges linked to the definition of the merging sequence. In this paper, we suppose that the merging sequence is given by the decision-making level (cf. Figure 1), where the CAVs negotiate using a global optimization function to decide on an effective passing order. The details of the decision-making level are out of the scope of this paper.

Among the approaches used to synchronize the motion of the CAVs w.r.t. passing sequence, one can cite the consensus-based approaches. The consensus-based control theory [10] offers the possibility to develop a formal approach to tackle the driving maneuver while taking into account the safety constraints. In [9], the authors proposed a cooperative on-ramp merging approach based on consensus-based control theory, where the passing sequence and motion coordination are performed to optimize the energy efficiency of the CAVs in formation. The main drawback of such approach is that it relies on on the strongly connected graph assumption. Approaches depending on less strong communication assumption using optimization algorithm can also be found in the literature related to on-ramp merging. In [11], the authors proposed an analytical closed-form solution based on an energy efficient online coordination of the vehicles at the merging zones. Other approaches based on the virtual mapping of the vehicles from the merging road to the main line can be found in [12]. The objective of this paper is to take advantage from the formation modeling using the virtual structure ability and the optimization approaches for motion synchronization to outperform the on-ramp merging scenario performed by the CAVs, while ensuring mainly the safety requirement, and also the smoothness of the performed maneuvers.

The main contribution of this paper is a safe and smooth on-ramp merging approach based on a Constrained Optimal Reconfiguration Matrix (CORM) algorithm. The first objective of the CORM algorithm is to adapt the inter-target distance matrix proposed in [13], originally created for open-world environment, to explicitly take into account the constraints imposed by the merging scenario (e.g., the road borders and the road centerline). This adaptation passes through the respect of the global reference path defined in the second level of the architecture given in Figure 1. The second objective of the proposed approach is to take advantage from the virtual structure approach ease to represent the formation in order to respect the passing order fixed by the decision-making level (cf. Figure 1). To this aim, a structure reconfiguration from the initial virtual shape toward the final desired one is proposed, while respecting the intra-formation safety.

III. Preliminaries and Problem Statement

This section is dedicated to highlight the adopted CAV formation modeling approach and to give a sum-up of the formation control initially proposed in [13], which is useful to understand the contribution proposed in this paper. The aim is to have a self-contained paper.

A. Preliminaries

In addition to this section where the used nomenclature in this paper is presented, please confer to Figure 2.

- $N \in \mathbb{N}$ is the number of the considered CAVs that are in the communication range, referred to individually by i, and $\mathcal{N} = \{1, ..., N\}$ is the set representing all the CAVs indices.
- The pose in the global frame $\{X_G, Y_G\}$ of V_i is defined by $X = [x, y, \theta]^T$ and its dynamic is referred to by $[\mathcal{V}, \delta]^T$ for linear velocity and steering angle, respectively.
- The coordinates of V_i w.r.t. the mobile reference frame centered on V_R are h_i and l_i for longitudinal and lateral coordinate respectively.
- $f_i = [h_i, l_i]^T$ is V_i coordinates in the formation, $F = [f_1, ..., f_N]$ is the coordinates of the formation composed of $N, N \in \mathcal{N}$ CAVs.
- The operators $EucDis\{V_i, V_j\}$ and $PerpDis\{V_i, V_j\}$ are Euclidean and perpendicular distance between the vehicle V_i and the vehicle V_j respectively.

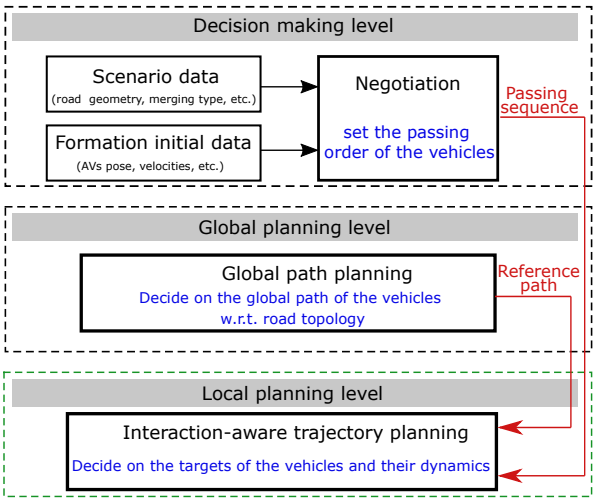

Fig. 1. Overall architecture on the different levels of decision and global/local path and trajectory planning.

- T_{d_i} is V_i virtual target used by the virtual structure approach to control the shape of the formation. For the knowledge of the reader, further details can be found in [7].

B. Modeling of the vehicle: kinematic model

The vehicle is modeled using the well-known tricycle model in [14]. A single front wheel replace the two front wheels, and it is placed in-between them. The equations of the kinematic model can be written as:

$$\begin{aligned} \dot{x} &= \mathcal{V}\cos(\theta) \\ \dot{y} &= \mathcal{V}\sin(\theta) \\ \dot{\theta} &= \mathcal{V}/l_b\tan(\delta) \end{aligned} \tag{1}$$

with $X = [x, y, \theta]^T$, l_b, $\mathcal{V}$ and δ are the vehicle's pose, its wheelbase, linear velocity and steering angle respectively. The latter is expressed as $\delta = \arctan(l_b C_c)$ where $Cc = 1/R$, with R is the radius of the road and Cc its curvature.

To achieve the dynamic $[V, \delta]$, we use a standard control law that permits the convergence of the vehicle's state vector toward the defined set-points. Since the control law is not in the scope of this paper, this part will not be developed in what follows. .

C. Formation modeling: Frenet based model

This paper uses the virtual structure approach formalism developed in [13] to model the formation composed by the N CAVs under the communication range (cf. Figure 2). Each CAV, part of the formation, can be characterized by its desired dynamic target to reach at each sample time T_{d_i}. In order to locate T_{d_i} w.r.t. the reference vehicle V_R (cf. Figure 2, the reference vehicle in blue with the index R, the CAVs part of the formation in magenta and green with index i and j), it is proposed to use a Frenet reference centered on V_R. According to V_R pose X_R and its reference trajectory (cf. Figure 2, main line), T_{d_i} can be written by its longitudinal coordinate h_i and lateral coordinate l_i, $f_i = [h_i, l_i]^T, \forall i \in \mathcal{N}$ as shown in the Figure 2. The longitudinal coordinate represents the distance between V_R and T_{d_i} according to the tangent to V_R trajectory, while the lateral coordinate is computed based on the perpendicular line between $X_R(h_i)$ and its reference trajectory, and that passes through T_{d_i}, $l_i = PerpDist\{X_R(h_i), T_{d_i}\}$ (cf. Figure 2).

The kinematic model in eq. (1) is written in the global reference $\{X_G, Y_G\}$, thus a transformation from the mobile reference to the global reference is obtained with the following equations:

$$\begin{bmatrix} x_{T_i} \\ y_{T_i} \end{bmatrix} = \begin{bmatrix} x_R(h_i) \\ y_R(h_i) \end{bmatrix} + \begin{bmatrix} -l_i\sin(\theta_R(h_i)) \\ l_i\cos(\theta_R(h_i)) \end{bmatrix} \tag{2}$$

With $[x_{T_i}, y_{T_i}]^T$ is the target of V_i w.r.t. V_R's mobile reference frame. $[x_R(h_i), y_R(h_i)]^T$ and $\theta_R(h_i)$ are the reference vehicle V_R pose and orientation at h_i longitudinal distance from its current pose along its trajectory.

D. Dynamic Reconfiguration Matrix

For a cooperative merging scenario of a formation composed of N vehicles, $V_i, i \neq j, i \in \mathcal{N}$ vehicles are already on the main lane and $V_j, j \neq i, j \in \mathcal{N}$ vehicles can be located on the merging reference trajectory (cf. Figure 2). The merging maneuver as represented in Figure 2 consists then to reconfigure the shape of the formation from its initial geometry to its final one, while ensuring that the inter-targets distances are safe. F^{init}, F^{end} and $F(t)$, as given in eq. (3) represent the initial, final and instantaneous coordinates of the formation respectively.

$$\begin{cases} F^{init} = [f_1^{init^T}, ..., f_N^{init^T}]^T, \\ F^{end} = [f_1^{end^T}, ..., f_N^{end^T}]^T, \\ F(t) = [f_1(t)^T, ..., f_N(t)^T]^T, \end{cases} \tag{3}$$

$f_i^{init}, f_i^{end}, i \in \mathcal{N}$ are the coordinates of V_i in the initial and final formation, while $f_i(t), i \in \mathcal{N}$ are its instantaneous coordinates.

$e_{f_i} = [e_{h_i}, e_{l_i}]^T$ is the convergence error between the desired coordinates of V_i in the formation and the actual ones, it can be defined as:

$$\begin{cases} e_{f_i} = f_i^{end} - f_i(t), \\ f_i(t) = [h_i(t), l_i(t)]^T, \\ f_i^{end} = [h_i^{end}, l_i^{end}]^T, \end{cases} \tag{4}$$

The global error for a formation composed of N vehicles can be written as:

$$e_F = F^{end} - F(t) \tag{5}$$

The derivative expression of the error can be written as:

$$\dot{e}_F = g(e_{f_1}, ..., e_{f_N}) \tag{6}$$

In order to characterize the evolution of the reconfiguration from the initial shape to the desired one, while ensuring the respect of the minimum inter-target distance between the N CAVs part of the formation, it is proposed to impose a first order dynamic to eq. (6), which can be written:

$$\dot{e}_F = Ae_F \tag{7}$$

where $e_F = [e_{f_1}^T, ..., e_{f_N}^T]^T$ and $A^{N\times N}$ are the state vector and the inter-target distance matrix corresponding to a formation of N CAVs, respectively.

$$A = \begin{bmatrix} a_1 & a_{12} & \cdots & a_{1N} \\ -a_{12} & a_2 & \cdots & a_{2N} \\ \vdots & \vdots & \ddots & \vdots \\ -a_{1N} & -a_{2N} & \cdots & a_N \end{bmatrix} \tag{8}$$

The gains a_i on the diagonal with $\forall i \in N$ control the convergence rate of the error, while a_{ij} with $i \neq j | \forall i, j \in \{N \times N\}$ are related to the inter-target distance between T_{d_i} and T_{d_j}, to ensure the convergence of the formation toward its desired shape. For more details on how to choose the values of a_i and a_{ij}, in order to guarantee both asymptotic convergence of the vehicles towards their assigned targets

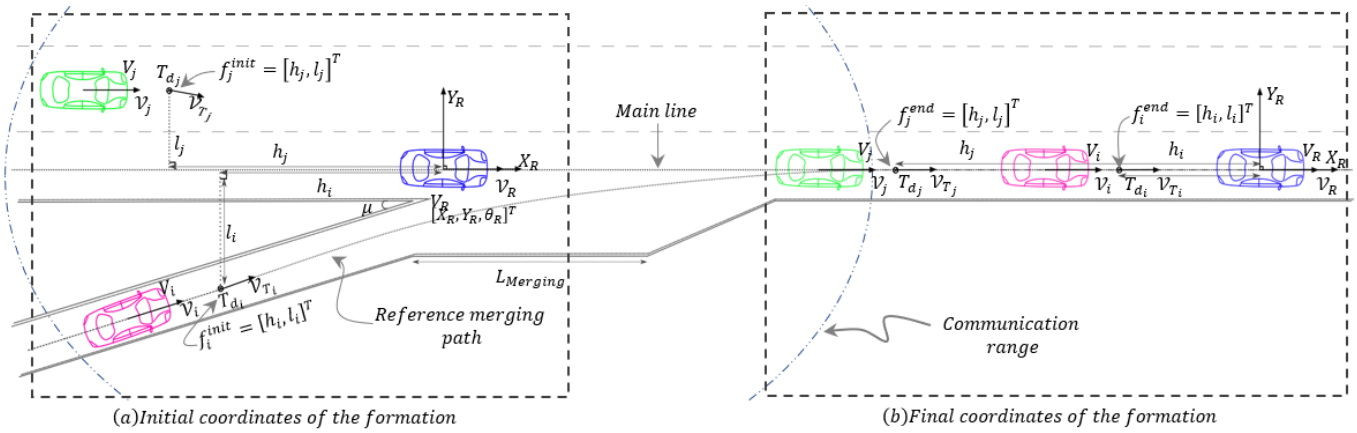

Fig. 2. The virtual structure approach used to model the formation and its reconfiguration to perform the merging maneuver. (a) The initial shape of the formation and its coordinates. (b) The final shape of the formation after the merging maneuver and its desired coordinates.

and to guarantee no collision between the vehicles during the reconfiguration phase, please refer to [13].

It is important to highlight that to avoid the collisions between the N CAVs composing the formation, the condition relating the minimum inter-distance and the gains of the matrix A must be satisfied. For the clarity of the paper, it is proposed to take the case of a formation composed of three CAVS, a_{ij} must be chosen as:

$$\|\frac{a_2 - a_3 + 2a_{23}}{a_{23} - a_3} e_{f_2} + e^{end}_{F_{23}}\| \geqq \underline{D}_T \tag{9}$$

where $e^{end}_{F_{23}} = EucDis\{f^{end}_2, f^{end}_3\}$ and $\underline{D}_T$ is the minimum safety distance between the CAVs.

The inter-target distance matrix proposed in [13] is designed for an open-world environment, where a reactive collision avoidance approach was used only against the other robots present in the environment. Nevertheless, in the proposed paper, it is targeted to deal with structured on-road environment, with road borders. It is thus important that the CAV reconfiguration takes into account these constraints.

IV. On-ramp cooperative merging for cooperative automated vehicles

In on-road environment, CAVs travel in a constrained environment, imposed by the road borders and the road geometry. As stated in Section II, the inter-target distance matrix proposed in [13] do not take environments with such constraints. In order to take these constraints into account, we propose a two-step approach (cf. Figure 3). First, through an optimization algorithm, we compute a constrained inter-target distance matrix. This latter generates the targets T_d for N CAVs part of the formation, that ensure the reconfiguration convergence from the initial configuration toward the desired final one (cf. Figure 2), while guaranteeing the respect of the safety distance between the CAVs. The geometry of the road (i.e., the road borders and the road center-line) is taken into account at this level using the objective function in eq. (10). In section IV-A, the details of this first step are presented.

The constrained optimization in the first step allows us to generate $\mathcal{M}$ (cf. Figure 4); an approximation of the global reference trajectory w.r.t. the objective function given in eq. (10). However, the targets T_d are not on the reference path, thus, we propose to project these targets using a Frenet reference w.r.t. the reference path to obtain the projected targets T_p. The dynamic of the projected targets T_p is similar to the one of T_d, which means that if the vehicles follow T_p correctly, we can guarantee that they will stay on their reference trajectory. However, their in-between distance profile will not be the same as if they follow T_d. Thus, it is proposed to impose a new dynamic to T_p to obtain $\bar{T}_p$. The latter makes sure that the vehicles are at the same safety distance as the one obtained with the constrained inter-target matrix when they approach the conflicting zone (cf. Figure 4). Section IV-B shows the details of the computation of the projected target and its dynamic.

A. Constrained Optimal Reconfiguration Matrix

The objective of the optimization algorithm presented in what follows is to compute the optimal constrained inter-target distance matrix w.r.t. eq. (10).

Since we aim to tackle constrained on-road scenarios, it is proposed to embed these constraints using the following cost function:

$$J_{a_{i,j}} = \sum_{k=0}^{T} \Bigg[w_i \Big[\frac{PerpDist(T_{d_i}(k)/T_{p_i}(k))}{PerpDist(T_{p_i}(k)/Border)} \Big]^2 + w_j \Big[\frac{PerpDist(T_{d_j}(k)/T_{p_j}(k))}{PerpDist(T_{p_j}(k)/Border)} \Big]^2 \Bigg] \tag{10}$$

Eq. (10) is composed of two terms: the first term takes into account the CAVs already in the main lane (referred to by the index i), it aims to minimize distance between V_i's reference path and T_{d_i}. while the second term related to the merging CAVs (referred to by the index j), considers the minimization of distance between T_{d_j} and its reference path (cf. Figure 4). w_i and w_j with $w \in \mathbb{R}$, correspond to the optimization weights balance between the two sub-criteria, the weight related to the merging CAV is higher to give the latter a sufficient flexibility w.r.t. to the CAV already on the main line. $T_{d_{i,j}}$ and $T_{p_{i,j}}$ are

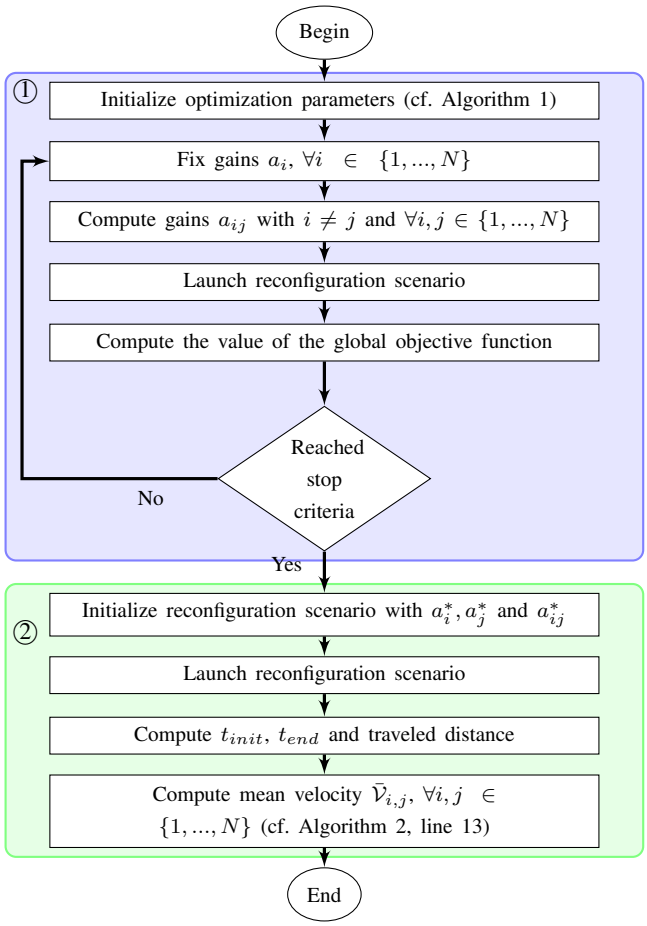

Fig. 3. The proposed CORM (Constrained Optimal Reconfiguration Matrix) flowchart. ① The optimization algorithm. ② The projection and mean velocity computation

the targets obtained with constrained inter-target distance matrix and their projected points respectively (cf. Figure 4, ①). $PerpDist(T_{d_{i,j}}(k)/T_{p_{i,j}}(k))$ are the perpendicular distances between T_d and its projected target w.r.t. to the reference path, while $PerpDist(T_{p_{i,j}}(k)/Border)$ are the perpendicular distances between the projected target and the road border, used to normalize the objective function (cf. Figure 4, ①).

In Figure 3, ①, the details of the optimization process are proposed. As can be seen in eq. (10), through the optimization algorithm, it is aimed to compute the diagonal gains of A (i.e., the reconfiguration convergence rate from the initial formation coordinates toward its desired final one). Since the objective function is non-linear, the optimization algorithm (cf. Algorithm 1, Inputs) needs the optimization boundaries $[a_{i,j_{min}}, a_{i,j_{max}}]^T$ and the starting point $[a_{i_0}, a_{j_0}]^T$. The anti-diagonal gains of A in charge of the inter-target distances are computed using eq. (9). The full merging scenario is launched with a constant reconfiguration matrix A. The latter is composed of the gains fixed by the optimization algorithm (cf. Figure 3). The data related to the merging scenario are used to compute the objective function in eq. (10). The latter is used to judge of the stop criteria; when the minimum of the cost function is reached, the optimization algorithm returns the optimal values of the gains a_i^* and a_j^*, $\forall i, j \in \{1, ..., N\}$.

Algorithm 1: Optimization Algorithm

Input : $GlobalInput$ Scenario data
$[a_{i_{min}}, a_{i_{max}}]^T$ boundaries of the gain a_i
$[a_{j_{min}}, a_{j_{max}}]^T$ boundaries of the gain a_j
$[a_{i_0}, a_{j_0}]^T$ start point of the optimization
$ObjectiveFunction$ the objective function in eq. (10)
Output : $[a_i^*, a_j^*]^T$ optimal values of the gains a_i and a_j

1 $MergingData \leftarrow [PerpDist\{T_{d_i}, \bar{T}_{d_i}\}, PerpDist\{T_{d_j}, \bar{T}_{d_j}\}, PerpDist\{\bar{T}_{d_i}, Border\}, PerpDist\{\bar{T}_{d_j}, Border\}]^T$
2 **while** $(StopCriteria \neq True)$ **do**
3 $[a_i, a_j]^T \leftarrow Fixe([a_{i_0}, a_{i_0}]^T, [a_{imin}, a_{imax}]^T, [a_{jmin}, a_{jmax}]^T)$
4 $MergingData \leftarrow MergingScenario(GlobalInput, a_i, a_j)$
5 $T \leftarrow length(MergingData)$
6 **forall** $t \in [0, T]$ **do**
7 $Cost(t) \leftarrow ObjectiveFunction(MergingData(t))$
8 $GlobalCost \leftarrow Sum(Cost)$

B. Safe and feasible local trajectory planning

The following section aims to explain the projection approach based on a Frenet reference frame that ensures the respect of the global reference path imposed by the global path planner (cf. Figure 1), in addition to the computation of the velocity profile imposed to the projected target T_p to ensure the safety, feasibility and smoothness of the merging maneuver.

1) Global reference path aware target: The constrained optimal inter-target distance matrix allows us to respect the road constraints while ensuring CAVs'safety. However, the generated targets T_d using A in eq. (8) are not part of the reference merging path (cf. Figure 4, ①). In order to ensure this requirement, it is proposed to use the reference path as a guiding system for the vehicle and compute its effective target T_p w.r.t. this latter (cf. Figure 4,①).

Each target T_d of the merging CAV is projected w.r.t. the reference merging path using a Frenet reference frame $[X_f, Y_f]$ (cf. Figure 4) to obtain T_p. The lines 10 and 11 in Algorithm 2 and eq. (2) details the transformation from the mobile reference centered on V_R to the global reference $[X_G, Y_G]$, in addition to the projection function that uses the reference merging path and $T_d \in \mathcal{M}$ to obtain T_p (cf. Figure 4,①).

2) Safe and feasible velocity profile : The projected target T_p has a similar dynamic as T_d. However, in order to draw full advantages from the constrained optimal inter-target distance matrix in terms of safety formal insurance (cf. eq. (9)), it is proposed to use the latter to compute the necessary mean velocity that must be imposed to the CAVs, such that they enter the conflicting zone (cf. Figure 4, ②) at the same moment as if they have followed T_d.

Before the presentation of the imposed dynamic details, for the clarity and the understanding of the paper, it is proposed to define the conflicting zone. The conflicting zone (cf. Figure 4,②) defines the area where a collision between the merging CAV and the CAVs on the main line may occurs. $\mathcal{P}_{merging}$ defines the position of the merging CAV where the surrounding circles of the merging CAV V_i and the CAV V_i may overlap, resulting in a collision. The points A , B , C and D define the limits of the conflicting zone,

where A is the pose of the merging where a collision may occurs, B is related to the limits of the main line. The point D defines the end of the merging zone, while C is its projection w.r.t. the main line limit (cf. Figure 4, ②).

Based on the definition of the conflicting zone, it is proposed to compute the mean velocity $\bar{\mathcal{V}}_{i,j}$ where i, j are the indices of the vehicles V_i and V_j respectively (cf. Figure 4, ②), such that the in-between distance respect the following:

$$EucDist\{\bar{T}_{p_j}(t_{end}), \bar{T}_{p_i}(t_{end})\} = EucDist\{T_{d_j}(t_{end}), T_{d_i}(t_{end})\} \quad (11)$$

where t_{end} is the time when the pose $\mathcal{P}_{merging}$ is reached by the merging CAV. $EucDist\{T_{d_j}(t_{end}), T_{d_i}(t_{end})\}$ represents the Euclidean distance between the targets T_{d_i} and T_{d_j} generated by A in eq. (8) for the CAVs V_i and V_j, while $EucDist\{\bar{T}_{p_j}(t_{end}), \bar{T}_{p_i}(t_{end})\}$ (cf. Figure 4, ②) is the in-between Euclidean distance between the targets with the imposed dynamic $\bar{\mathcal{V}}_i$ and $\bar{\mathcal{V}}_j$ for the CAV V_i and V_j, respectively.

The mean velocity $\bar{\mathcal{V}}_{i,j}$ where i, j are the indices of the vehicles V_i and V_j (cf. Figure 4, ②) is computed based on the line 13 in Algorithm 2, where t_{init} is the corresponding time when the reconfiguration was launched. A curvilinear distance formula is used to get the traveled distance by each CAVs between t_{init} and t_{end}.

In order to have the smoothest possible behavior w.r.t. the CAVs dynamics, it is proposed to use a sigmoid function to shape the velocity profile. This latter is used to create a velocity profile that goes from the CAV's initial velocity toward the mean velocity, and goes to the reference vehicle V_R velocity when the vehicle enters the main line. This choice is motivated by the sigmoid ability to smoothly control the convergence rate from an initial velocity to the final desired one. In other terms, using the sigmoid function permits us to impose a feasible and comfortable acceleration and deceleration profile to the CAVs.

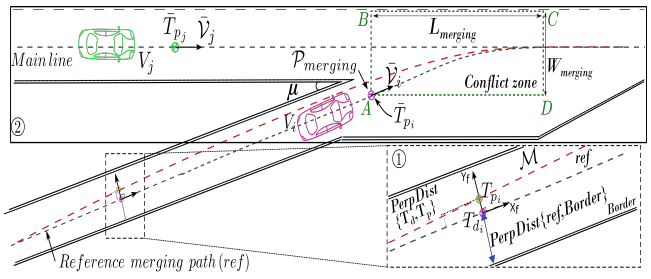

Fig. 4. Projection of T_{d_i} w.r.t. the reference trajectory

V. Simulation Results

In order to evaluate the efficiency of CORM in terms of its ability to guarantee safety and smooth vehicles' dynamics of the overall CAV, while performing the on-ramp merging task, a first scenario is proposed. It aims to perform the merging maneuver with a formation of CAVs. Then, a comprehensive summary of several conducted simulations is presented in Table II.

Algorithm 2: Projections and computation of the imposed dynamic

Input : $GlobalInput$ Scenario data
a_i^*, a_j^*, a_{ij}^* optimal gains of the reconfiguration matrix (cf. Algorithm 1)
Output : $\bar{\mathcal{V}}_{i,j}$ the mean velocity of the vehicles V_i and V_j

1 $k \leftarrow 1$
2 $\mathcal{F}(k) \leftarrow F^{init}$
3 $\varepsilon(k) \leftarrow \mathcal{F}^{end} - \mathcal{F}(k)$
4 $Buffer_R \leftarrow ReferenceTrajectory(V_R)$
5 $Buffer_{i,j} \leftarrow ReferenceTrajectory(V_i, V_j)$
6 **while** $(\varepsilon(k) \neq 0)$ **do**
7 $k \leftarrow k + 1$
8 $\mathcal{F}(k) \leftarrow DynamicReconfiguration(\mathcal{F}^{end}, \mathcal{F}(k-1))$
9 $\varepsilon(k) \leftarrow \mathcal{F}^{end} - \mathcal{F}(k)$
10 $T_{d_{i,j}}(k) \leftarrow Transform(Buffer_R, \mathcal{F}(k), X_{V_R})$
11 $T_{p_{i,j}}(k) \leftarrow Projection(Buffer_{i,j}, T_{d_{i,j}})$
12 $X_{V_{i,j}}(k) \leftarrow Control(X_{V_{i,j}}(k-1), T_{p_{i,j}}(k))$
13 $\bar{\mathcal{V}}_{i,j} = \frac{CurviDist\{V_{i,j}(1,k)\}}{t_{end} - t_{init}}$

TABLE I
The values of the inputs of the CORM algorithm

Inputs	Values
Initial formation coordinates $[m]$	$\begin{pmatrix} 0 & -40 & -50 \\ 0 & 0 & 9.2 \end{pmatrix}$
Final formation coordinates $[m]$	$\begin{pmatrix} 0 & -80 & -40 \\ 0 & 0 & 0 \end{pmatrix}$
$\mathcal{V}_{1,2,3}[m/s]$	$[19.4, 19.4, 19.4]$
$[a_{2min}, a_{2max}]^T$	$[-0.4, 0.1]$
$[a_{3min}, a_{3max}]^T$	$[-0.4, -0.05]$
$[a_{2_0}, a_{3_0}]^T$	$[-0.25, -0.25]$
$[w_2, w_3]^T$	$[1, 4]$
$[a_2^*, a_3^*]^T$	$[-0.1228, -0.365]$
$\underline{D}_T[m]$	12

A. On-ramp merging in formation

In the following simulation, it is aimed to perform a merging maneuver with a formation of three CAVs. The considered merging scenario is an on-ramp merging road with an incidence angle $\mu = 10°$, $V1$ (i.e., the reference vehicle V_R) is placed in the main line, so as V_2. The third vehicle V_3 is initially placed in the secondary on-ramp merging road (cf. Figure 2). The initial formation shape is triangular, consequently at the end of the reconfiguration phase the aim is to put the three vehicles in a linear shape to form a convoy. Table I resumes the scenario inputs. The video of the simulation can be found in https://youtu.be/UM2cLt74pVM

The minimum distance between the CAVs is $\underline{D}_T$, it is computed using the following equation:

$$\underline{D}_T = (R_i + R_j) + offset \quad (12)$$

where R_i and R_j are the radius of the circles that surround the vehicles V_i and V_j, and $offset$ is the safety distance to avoid rear-end collision.

The reconfiguration of the triangular shape toward the final desired linear one is illustrated in Figure 5. The formation defined by its initial shape coordinates passes through a reconfiguration phase, where V_3 is behind V_2. To be able to place the merging vehicle between V_1 and V_2 as desired w.r.t. the final coordinates of the formation, the $EucDist(V_1, V_2)$ needs to increase. The intermediate formation showcases the pose of the three AVs in the conflict zone. As expected, $EucDist(V_1, V_2)$ has increased to make space for V_3 in the convoy. In the second phase, after the convergence of the

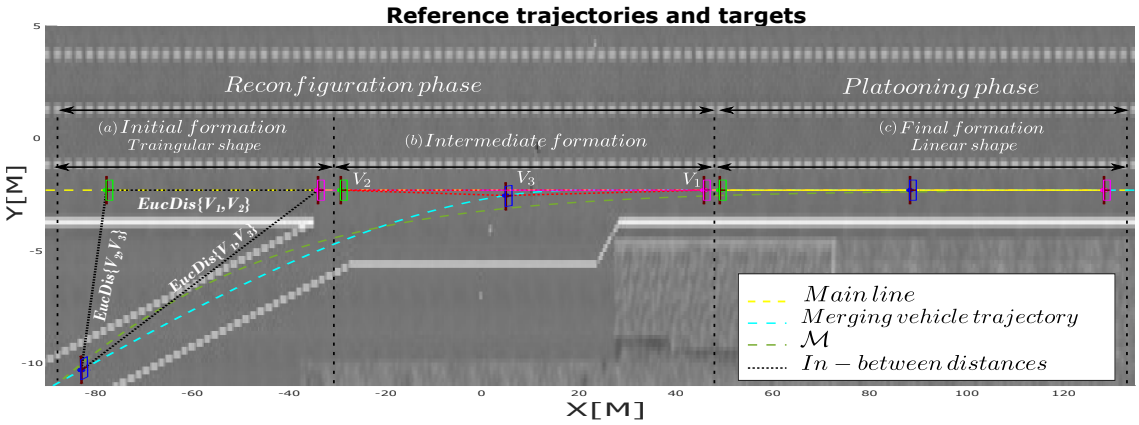

Fig. 5. Evolution of the virtual structure shape while the on-ramp is being performed

formation toward its desired final shape, the vehicles form a linear shape, where the desired in-between distances are respected.

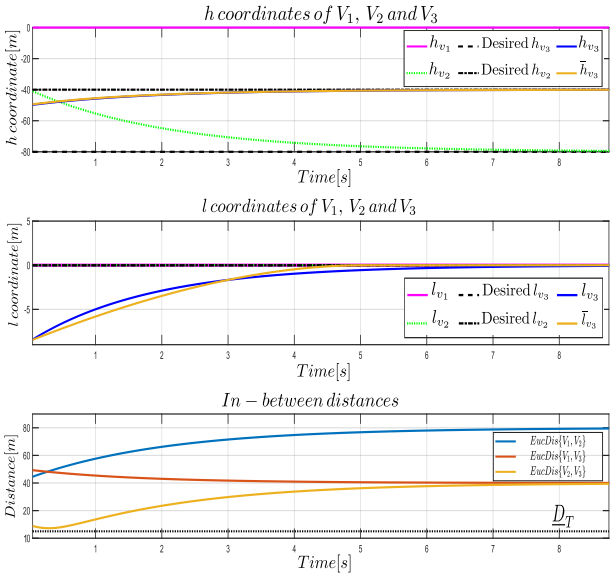

Fig. 6. Formation coordinates and in-between distances evolution

To evaluate the capability of the CORM algorithm in terms of safety and convergence errors, it is proposed to study the evolution of the formation coordinates and the in-between distances profiles in Figure 6. A first order asymptotic convergence from the initial values of the longitudinal and lateral coordinates toward their final ones can be noticed. As for the minimum distances, the in-between distances profiles are always greater than $\underline{D}_T$. The in-between distances when the vehicles are in the conflicting zone (i.e., l_{v_3} with projections greater than 5m) is greater than $20m$. The final in-between distances meet the safety requirement for a convoy formation; $EucDist(V_i, V_j) = 2[s] \times \mathcal{V}_{i,j}[m/s] = 40m$.

In Figure 7, the linear velocity, the longitudinal and lateral accelerations are presented for each vehicle. As expected, the velocity of the vehicle V_2 decreases at the beginning of the scenario to make space for V_3, before it increases to make sure that V_2 meets the velocity requirement in the platooning

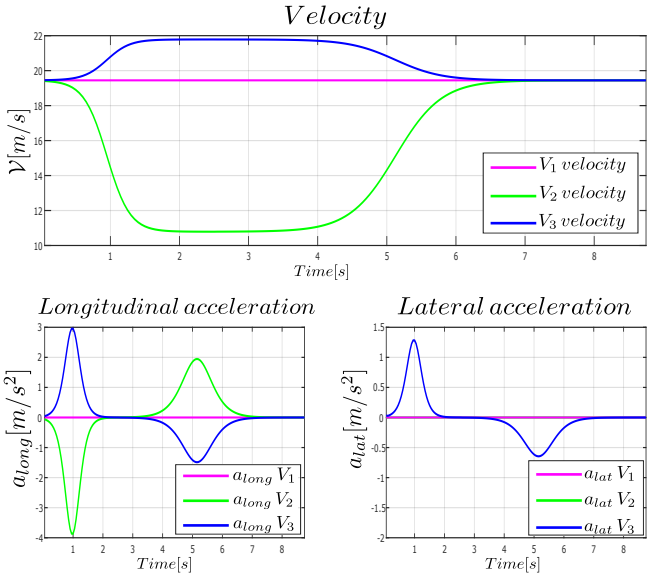

Fig. 7. Velocity and acceleration profiles

phase. As for V_3, its velocity increases at the beginning to enter the highway centerline while respecting the safety distances. A decreasing can be noticed around $4s$ to follow the convoy velocity (fixed to $19.4m/s$ - $70km/h$). Figure 7 confirms that the longitudinal and lateral accelerations respect the maximum and minimum authorized acceleration (i.e., $-4m/s^2$ for deceleration and $3m/s^2$ for acceleration). We can conclude with the help of the velocity and acceleration profiles of each vehicle that the merging maneuver is smooth and comfortable.

B. Influence of the projection phase on the CORM efficiency

This subsection is dedicated to validate more intensively the proposed approach, while emphasizing mainly the viability of the projection phase for different environments' structure (several values of μ (cf. Figure 2), and dynamic of the CAVs).

For a range of incidence angles between $\mu = 10°$ and $\mu = 30°$ with $\Delta\mu = 10°$ step each time, we test the performance of CORM for velocity between $5m/s$ and $15m/s$ with an

TABLE II

THE SUMMARY RESULTS OF THE CONDUCTED SIMULATION FOR A VARIABLE INCIDENCE ANGLE μ AND CAVS VELOCITY $\mathcal{V}$

μ[deg]	10			20			30		
$\mathcal{V}_R[m/s]$	5	10	15	5	10	15	5	10	15
$[\mathcal{V}_{2min}, \mathcal{V}_{2max}][m/s]$	[4.36, 5]	[8.73,10]	[13.45, 15]	[4.21, 5]	[8.49,10]	[13.26, 15]	[4.13, 5]	[8.35,10]	[13.06,15]
$[\mathcal{V}_{3min}, \mathcal{V}_{3max}][m/s]$	[5,5.59]	[10,11.125]	[15,16.80]	[5,5.824]	[10,11.6316]	[15,17.43]	[5,6.10]	[10,12.10]	[15,18.14]
$[a_{2min}, a_{2max}]_{long}[m/s^2]$	[-0.29, 0.15]	[-0.60, 0.29]	[-0.70, 0.35]]	[-0.35, 0.18]	[-0.68, 0.34]	[-0.78, 0.53]	[-0.38,0.19]	[0.70,0.37]	[-0.87,0.44]
$[a_{2min}, a_{2max}]_{lat}[m/s^2]$	[0,0]	[0,0]	[0,0]	[0,0]	[0,0]	[0,0]	[0,0]	[0,0]	[0,0]
$[a_{3min}, a_{3max}]_{long}[m/s^2]$	[-0.76,1.52]	[-1.66, 2.02]	[-1.14,2.27]	[-0.570,1.07]	[-1.66, 2.02]	[-1.54,2.92]	[-0.65,1.39]	[-1.31,2.55]	[-2.00,2.75]
$[a_{3min}, a_{3max}]_{lat}[m/s^2]$	[-0.29,0.74]	[-0.39,0.80]	[-0,74,1.38]	[-0.84,0.75]	[-1.02,0.96]	[-1.60,1.59]	[-1.56,1.55]	[-2.23,1.94]	[-3.63,2.53]
$\underline{D}[m]$	21.66	21.80	23.30	24.75	24.01	23.30	28.70	27.30	25.725
$Error_{max}[m]$	0.52	0.73	0.78	0.85	0.88	0.92	1.10	1.13	1.14

increase of $5m/s$ each time. For all the simulations, the inputs of the CORM algorithm are the same as in Table I. The results of the conducted simulations are summarized in Table II.

According to the performed simulations, it is important to emphasize that the safety of CAVs is always ensured. The minimum inter-vehicle distance in the conflicting zone $\underline{D_T}$ is always greater than $20m$. The metric $Error_{max}$ is the maximum distance between T_d and $\bar{T}_p$. This latter is lower than $1.5m$ (distance between the centerline and the road border), in other terms, T_d is never out of the road borders.

To evaluate the smoothness of the merging, it is proposed to discuss the obtained velocity and acceleration profiles w.r.t. variable velocity and incidence angle. The velocity profiles are similar to the one represented in Figure 7, with a sigmoid shape that makes $\mathcal{V}_2$ decrease toward $\bar{\mathcal{V}}_2$ and $\mathcal{V}_3$ increase toward $\bar{\mathcal{V}}_3$ in beginning to make space for V_3. $\mathcal{V}_2$ and $\mathcal{V}_3$ decreases and increases respectively toward $\mathcal{V}_R$ to form the final desired platoon. As for the acceleration, the lateral and the longitudinal behavior respect the limits of feasibility and comfort (i.e., $-4m/s^2$ for the deceleration and $3m/s^2$ for the acceleration).

VI. CONCLUSION AND PERSPECTIVES

This paper proposed a safe and smooth on-ramp merging approach based on a Constrained Optimal Reconfiguration Matrix (CORM) algorithm. The CORM framework can be summarized as a two steps approach: (1) An optimization algorithm to include explicitly the environment constraints. This step aims to compute the convergence rate imposed to the constrained inter-target distance matrix A, in charge of the reconfiguration of the virtual structure from its initial shape toward the final desired shape to perform the merging maneuver. (2) A projection based approach with safe and suitable dynamic. This step ensures that the dynamic targets given to each CAV, to perform the addressed scenario, are feasible and respect the global reference path. The targets obtained in step (1) are projected using a Frenet reference frame attached to the global reference path to ensure the respect of this latter, while a smooth velocity profile based on a sigmoid shape was used to guarantee the smoothness of the maneuver. The evaluation of the CORM algorithm was conducted in simulated environment, where the approach capability to guarantee the respect of the safety criteria was demonstrated, even for challenging and high velocity merging scenario. The approach viability for different incidence angles μ of the merging road and dynamics of the formation were demonstrated through extensive simulations. The future works based on the CORM algorithm will mainly consider its implementation on real vehicles available in the laboratory.

REFERENCES

[1] S. Mariani, C. Giacomo and F. Zambonelli, Coordination of autonomous vehicles: taxonomy and survey, ACM Computing Surveys (CSUR), vol 54, pp. 1-33, 2021.

[2] A. Vahidi and A. Sciarretta, Energy saving potentials of connected and automated vehicles, Transportation Research Part C: Emerging Technologies, vol 95, pp. 822-843, 2018.

[3] N. Chen, B. van Arem, T. Alkim and M. Wang, A Hierarchical Model-Based Optimization Control Approach for Cooperative Merging by Connected Automated Vehicles, in IEEE Transactions on Intelligent Transportation Systems, vol. 22, no. 12, pp. 7712-7725, 2017.

[4] Z. Wang, Y. Bian, S. E. Shladover, G. Wu, S. E. Li and M. J. Barth, A Survey on Cooperative Longitudinal Motion Control of Multiple Connected and Automated Vehicles, in IEEE Intelligent Transportation Systems Magazine, vol. 12, no. 1, pp. 4-24, 2020.

[5] L. Chen and C. Englund, Cooperative Intersection Management: A Survey, in IEEE Transactions on Intelligent Transportation Systems, vol. 17, no. 2, pp. 570-586, 2016.

[6] S. E. Li, Y. Zheng, K. Li, and J. Wang, An overview of vehicular platoon control under the four-component framework. In IEEE IV, pp. 286-291, 2015.

[7] A. Benzerrouk, L. Adouane and P. Martinet, Stable navigation in formation for a multi-robot system based on a constrained virtual structure, In Robotics and Autonomous Systems, vol. 62, pp.1806-1815, 2014.

[8] H. Xu, S. Feng, Y. Zhang and L. Li, "A Grouping-Based Cooperative Driving Strategy for CAVs Merging Problems," in IEEE Transactions on Vehicular Technology, vol. 68, no. 6, pp. 6125-6136, 2019.

[9] Z. Wang, G. Wu, K. Boriboonsomsin, M.J. Barth, K. Han, B. Kim, and P. Tiwari, Cooperative Ramp Merging System: Agent-Based Modeling and Simulation Using Game Engine, SAE International Journal of Connected and Automated Vehicles, 2019.

[10] W. REN, Consensus strategies for cooperative control of vehicle formations. IET Control Theory and Applications, vol. 1, no 2, p. 505-512, 2007.

[11] J. Rios-Torres and A. A. Malikopoulos, Automated and Cooperative Vehicle Merging at Highway On-Ramps, in IEEE Transactions on Intelligent Transportation Systems, vol. 18, no. 4, pp. 780-789, 2017.

[12] M. Graf, O. Speidel, A. Kaushik, T. Phan-Huu, A. Wedel, K. Dietmayer, Trajectory Planning for Automated Driving in Intersection Scenarios using Driver Models, In 5th ICRA, 2020.

[13] J. Vilca, L. Adouane and M. Youcef, Stable and Flexible Multi-Vehicle Navigation Based on Dynamic Inter-Target Distance Matrix, IEEE Transactions on Intelligent Transportation Systems, vol 20, pp. 1416-1431, 2019.

[14] A. De luca, G. Samson and C. Samson, Feedback control of a nonholonomic car-like robot, in Robot Motion Planning and Control, ed J.P. Laumond, vol 229, pp. 171-253, 1998.